

Supplementary Materials for

Experimental realization of deep-subwavelength confinement in dielectric optical resonators

Shuren Hu*, Marwan Khater, Rafael Salas-Montiel, Ernst Kratschmer, Sebastian Engelmann, William M. J. Green, Sharon M. Weiss*

*Corresponding author. Email: shuren.hu@gmail.com (S.H.); sharon.weiss@vanderbilt.edu (S.M.W.)

Published 24 August 2018, *Sci. Adv.* **4**, eaat2355 (2018)
DOI: 10.1126/sciadv.aat2355

This PDF file includes:

Fig. S1. Design of photonic crystal cavity in an FDTD simulation.

Fig. S2. Resonance mode profile.

Fig. S3. Broadband transmission spectrum of bowtie photonic crystal cavity shown in Fig. 3D.

Fig. S4. SEM image and transmission of the bowtie photonic crystal cavity characterized by NSOM.

Fig. S5. Position-dependent electric energy distribution in the central cavity unit cell of the silicon bowtie photonic crystal.

Table S1. Calculated mode volume (V_m) and measured quality factor (Q) of different photonic crystal (PhC) cavities including the bowtie photonic crystal cavity presented in this work.

Table S2. NSOM-measured mode sizes of plasmonic structures in comparison to dielectric bowtie photonic crystal reported in this work.

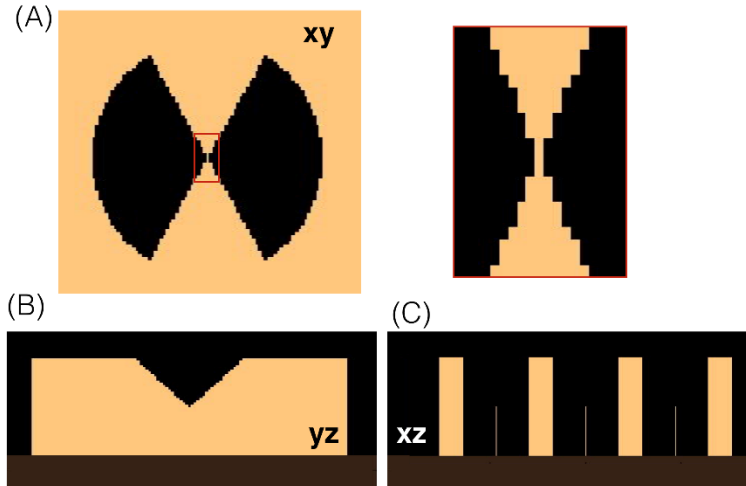


Fig. S1. Design of photonic crystal cavity in an FDTD simulation. (A) Top view of the meshed center cavity unit cell. The magnified image of the red boxed region shows the bowtie tip is connected by a 4 nm silicon bridge. (B) Thickness modification at the bowtie tip. The thickness of the silicon slab at the bowtie tip is half that of the full slab thickness, and the thickness linearly increases to the full slab thickness over a distance equal to half the radius of the bowtie (75 nm). (C) Side view at xz plane. The thicker silicon rectangles are the regions between air holes, and the thin wires with half height are the bowtie connection regions. (B) and (C) confirm the bowtie tip is connected.

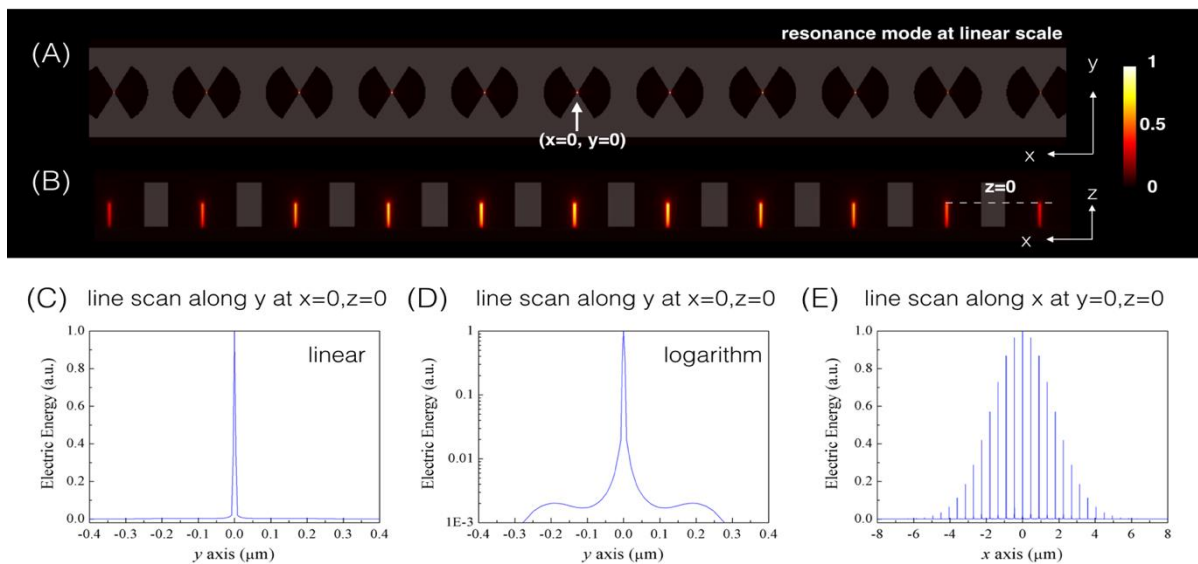


Fig. S2. Resonance mode profile. (A - B) The same electric energy distribution as Fig. 2E-F but here shown on a linear scale. (C) and (D) Linear and logarithm plot of electric energy distribution at the resonance wavelength along a vertical slice through the center of the bowtie photonic crystal cavity showing extreme energy localization. (E) Electric energy profile at the resonance wavelength along a horizontal slice through the center of bowtie photonic crystal cavity showing a gradual modulation of the electric energy from cavity center to mirror edges.

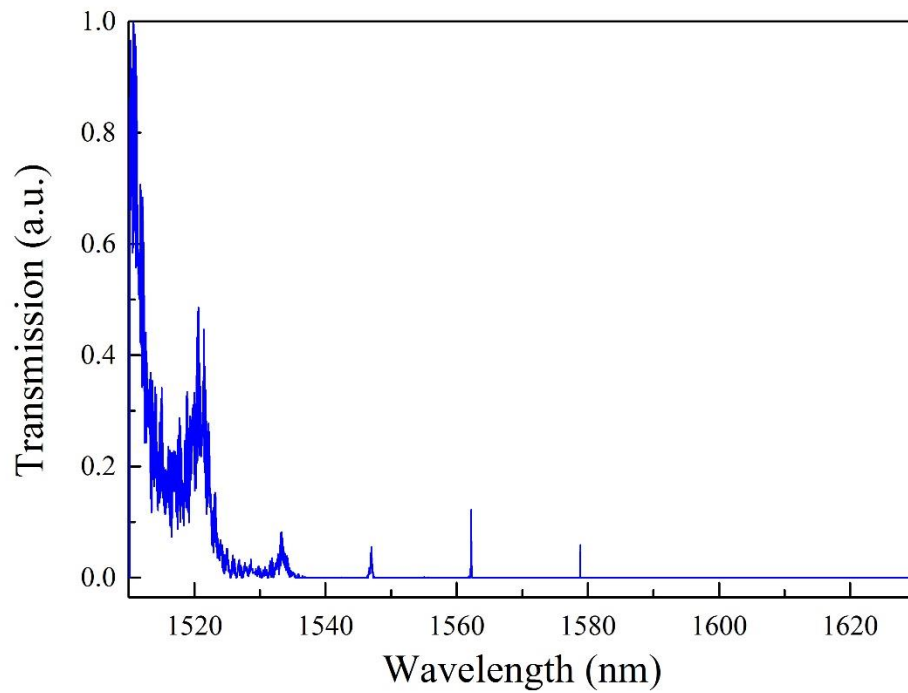


Fig. S3. Broadband transmission spectrum of bowtie photonic crystal cavity shown in Fig. 3D. The transmission of the resonance peak is relatively low compared to the photonic band edge transmission.

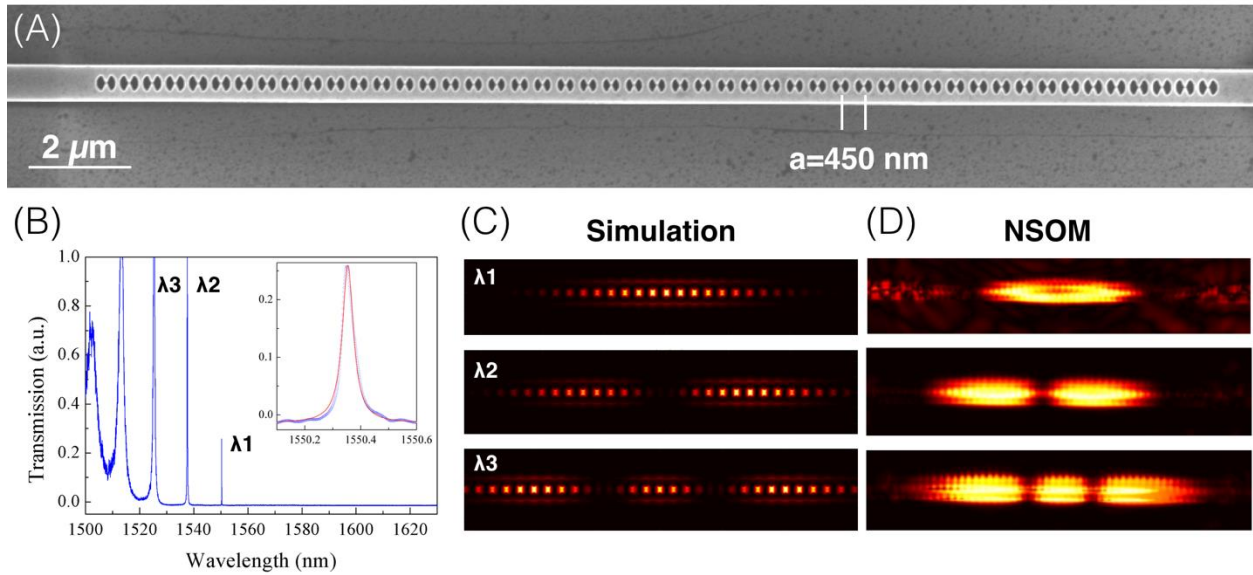


Fig. S4. SEM image and transmission of the bowtie photonic crystal cavity characterized by NSOM. (A) SEM image of bowtie photonic crystal cavity that is measured with NSOM. The structure has 20 taper unit cells and 5 mirror unit cells. The lattice spacing is 450 nm. The radii of the center and mirror unit cells are measured to be 145 nm and 185 nm, respectively. The width of the waveguide is measured to be 680 nm. (B) Transmission of photonic crystal shown in (A). The Q factor of the fundamental mode is 30,000, which is lower than that reported for the structure in Fig. 3 due to the reduced number of mirror unit cells that decreases optical confinement in the cavity. (C-D) Simulated electric energy distribution at 15 nm above silicon surface and corresponding NSOM measurement of the fundamental, 2nd and 3rd order resonances.

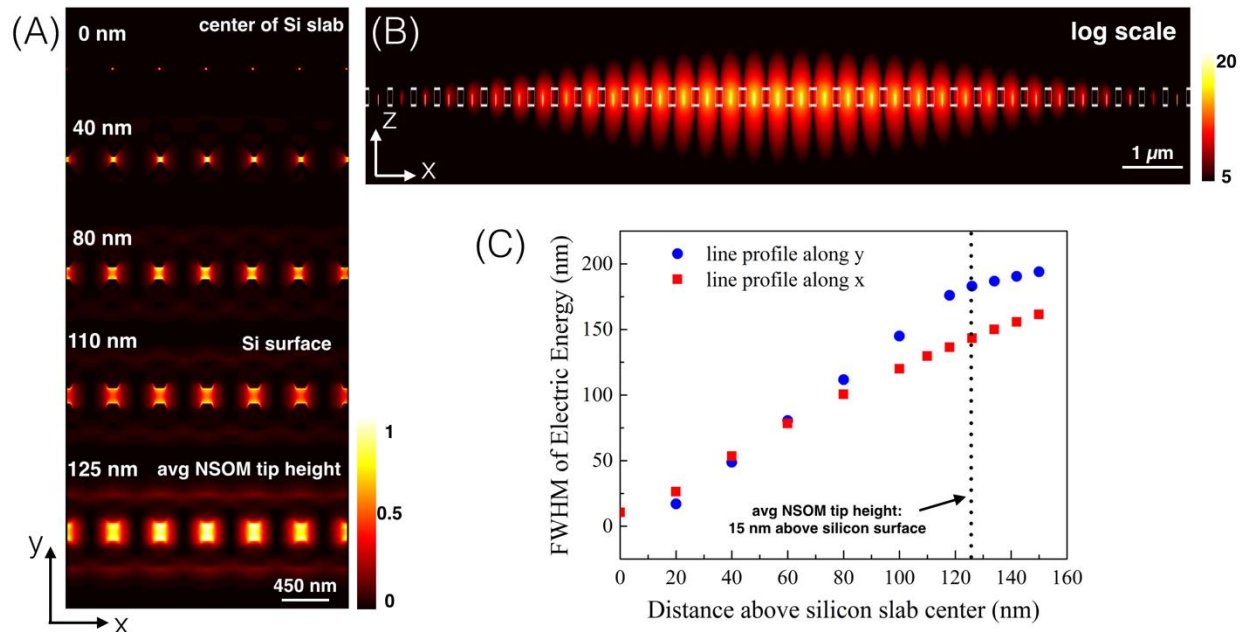


Fig. S5. Position-dependent electric energy distribution in the central cavity unit cell of the silicon bowtie photonic crystal. (A) Series of electric energy profiles inside the silicon slab and at different heights above the top surface. (B) Log plot of the photonic crystal cavity resonance mode in the xz plane at $y = 0$. Compared to the linear plot in **Fig. 2F**, plotting the natural logarithm of $|E^2|$, makes it easier to visualize that although the optical energy is well-confined at the bowtie tip, there is an energy tail that extends above the silicon surface. The NSOM tip is sensitive to the energy tail above (0-30 nm) the silicon surface. (C) The size of the electric energy localization in the bowtie unit cell is estimated as the full-width-at-half-maximum of the electric energy profile. This characteristic size increases with the distance from the center of the silicon slab. The characteristic size of the electric energy distribution in the bowtie unit cell along x and y is calculated to be approximately 143 nm and 183 nm, respectively, at a distance of 15 nm above the surface, which corresponds to the average distance at which the NSOM measures the electric energy.

Table S1. Calculated mode volume (V_m) and measured quality factor (Q) of different photonic crystal (PhC) cavities including the bowtie photonic crystal cavity presented in this work. The 2D PhC with L3 defect [28], 2D PhC heterostructure [29], dielectric mode nanobeam [22,23], and connected bowtie nanobeam localize light primarily in silicon while the slotted nanobeam [24] and the bowtie nanobeam with disconnected bowtie tips (i.e., air gap between dielectric bowtie tips – here we assume a similar Q would be measured from a bowtie photonic crystal with disconnected bowtie tips as the bowtie photonic crystal with connected bowtie tips experimentally demonstrated in this work) localize light primarily in air. (Images reproduced with permission from respective references).

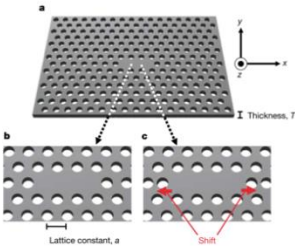
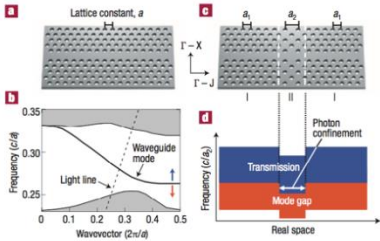
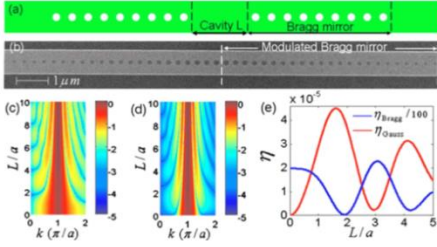
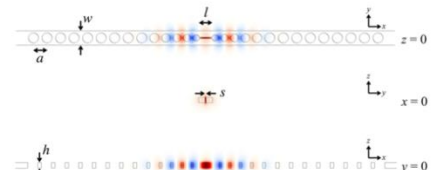
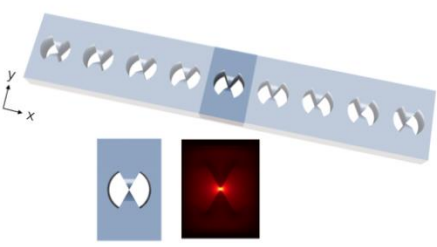
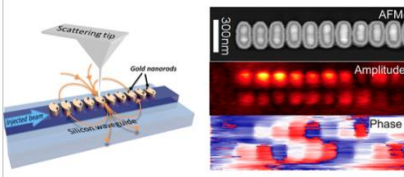
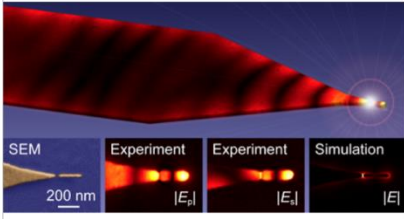
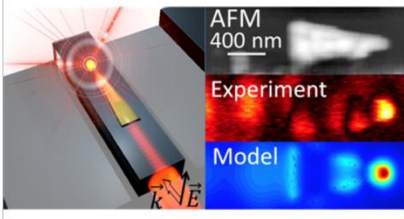
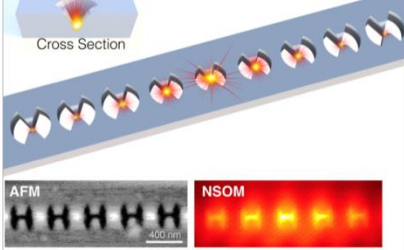
2D PhC: L3		$V_m: 0.71 (\lambda/n_{\text{Si}})^3$ $Q: 45,000$ $Q/V_m: 63,087$
2D PhC: heterostructure		$V_m: 1.2 (\lambda/n_{\text{Si}})^3$ $Q: 600,000$ $Q/V_m: 500,000$
Dielectric mode nanobeam		$V_m: 0.7\text{--}2 (\lambda/n_{\text{Si}})^3$ $Q: 80,000\text{--}720,000$ $Q/V_m: 500,000\text{--}700,000$
Slotted nanobeam		$V_m: 0.0096 (\lambda/n_{\text{air}})^3$ $Q: 140,000$ $Q/V_m: 1.4 \times 10^7$
Bowtie nanobeam (this work)		$V_m: 1.6 \times 10^{-4} (\lambda/n_{\text{air}})^3$ $Q: 100,000$ $Q/V_m: 6.25 \times 10^8$ $V_m: 6.9 \times 10^{-3} (\lambda/n_{\text{Si}})^3$ $Q: 100,000$ $Q/V_m: 1.4 \times 10^7$ (This work)

Table S2. NSOM-measured mode sizes of plasmonic structures in comparison to dielectric bowtie photonic crystal reported in this work. (Images reproduced with permission from respective references).

	<p>Plasmonic cavity gold particle chain λ: 1550nm</p>	<p>Measured E FWHM: $x \sim 100\text{nm}, y \sim 120\text{nm}$ (Ref. 30)</p>
	<p>Plasmonic cavity gold gap λ: 1550nm</p>	<p>Measured E FWHM: $x \sim 200\text{nm}, y \sim 200\text{nm}$ (Ref. 31)</p>
	<p>Plasmonic cavity gold triangle λ: 1550nm</p>	<p><u>Calculated $V_m \sim 0.00086 \mu\text{m}^3$</u> Measured $E ^2$ FWHM: $x \sim 130\text{nm}, y \sim 100\text{nm}$ (Ref.14)</p>
	<p>Silicon bowtie photonic crystal λ: 1561.21nm Simulated Q: 6.55×10^6 Measured Q: 1×10^5</p>	<p><u>Calculated $V_m \sim 0.0006 \mu\text{m}^3$</u> Measured $E ^2$ FWHM: $x \sim 267\text{nm}, y \sim 175\text{nm}$ (This work)</p>